FOCUSING PROPERTIES OF A SQUARE ELECTROSTATIC RAINBOW LENS DOUBLET

by

Igor N. TELEČKI* , Petar D. BELIČEV, Srdjan M. PETROVIĆ, and Nebojša B. NEŠKOVIĆ

Laboratory of Physics, Vinča Institute of Nuclear Sciences, University of Belgrade, Belgrade, Serbia

Scientific paper
DOI: 10.2298/NTRP1504239T

This is a study on the properties of a square electrostatic rainbow lens doublet. The said optical element consists of two square electrostatic rainbow lenses with the second lens axially rotated for 45 degrees with respect to the first one. The propagation of a proton beam with a kinetic energy of 10 keV through the doublet is in the focus of our analysis. The potential of the electrodes of both lenses is 2 kV. The electrostatic potential and the electric field components of the lens doublet are calculated using a 3-D computer code based on the method of moments. Spatial and angular distributions of protons propagating through the lens doublet, as well as the parameters defining beam quality, are investigated. As in the case of the single square electrostatic rainbow lens, the evolution of these distributions is determined by the evolution of corresponding rainbow lines, generated by the use of the theory of crystal rainbows. Our study shows that a beam core in the shape of a cusped square is formed by the spatial rainbow line that appears first. This rainbow line occurs during proton propagation through the first lens. The beam core retains the cusped square shape during the propagation through the second lens. The electrostatic field of the second lens causes the appearance of an additional spatial rainbow line, which encompasses the beam core and defines the outer border of the beam. This rainbow line constitutes the main difference between the cases of the lens doublet and a single lens.

Key words: electrostatic lense, particle beam dynamics, proton beam

INTRODUCTION

A conventional electrostatic quadrupole lens, widely used as an optical element in ion beam transport lines, contains four electrodes with the adjacent ones biased with potentials of the same magnitude but an opposite sign. If all the electrodes are biased with potentials of the same magnitude and sign, the optical element becomes a square electrostatic rainbow lens [1, 2]. Alternatively, it is referred to as an equally charged quadrupole lens [3]. The first term has been derived from the basic property of the lens, the appearance of a singular plane-to-plane mapping which results in an effect analogous to the meteorological rainbow effect [1]. The second term is related merely to the mode of biasing the lens.

The ion-optical properties of the square electrostatic rainbow lens used as a focusing element are presented in [1-3]. Biasing the electrodes of the lens with the time-varying potentials of the same magnitude and phase with an appropriate radio-frequency (RF) power supply turns the lens into an accelerating device [4, 5] which can be used for obtaining moderate energy gains within a low-energy ion beam experimental set-up. Although the resulting accelerating capacity is modest, the possibility of transforming an electrostatic quadrupole lens into an RF accelerating device at a relatively low cost is of considerable practical value.

The difference in the focusing properties of an electrostatic quadrupole lens and a square electrostatic rainbow lens is described systematically in [3]. It was determined that the focusing power of the former lens significantly exceeds (for approx. an order of magnitude) the focusing power of the latter lens. That is to be attributed to a significant difference in the magnitude of their transverse electrostatic fields. However, the rainbow lens possesses a unique feature qualitatively differentiating it from the quadrupole lens. The core of an ion beam passing through the first-mentioned lens stays confined within the rainbow line at very large distances after the lens itself, in the drift space. In other words, the rainbow lens exerts a specific freezing effect on the beam core [1].

Analysis of the accelerating properties of the square RF rainbow lens has shown that the acceleration takes place mainly within two accelerating gaps,

* Corresponding author; e-mail: tigor@vinca.rs

at the entrance and exit of the lens [4]. These are the gaps between the grounded electrodes and the cylindrical housing of the lens. It should also be noted that a quadrupole lens biased with an appropriate RF potential is used as a mass analyzer [6], rather than as an accelerating device.

A common practice when using quadrupole lenses is to group them into multiplets, *i. e*., systems of a few lenses rotated axially for 90 degrees relative to each other. This improves their optical characteristics, *e. g*., by achieving the net focusing effect along both transverse directions or by elimination of the astigmatism in the paraxial optics approach [7, 8].

Following this rationale, we have concentrated our study on the properties of a square electrostatic rainbow lens doublet in order to investigate how rainbow patterns change during ion beam propagation, along with some other optical parameters of the system. The results obtained should facilitate the answer to the question concerning the properties of the lens doublet in comparison to the properties of a single square electrostatic rainbow lens, as well as the issue of the specificities of the rainbow patterns appearing in the system. The answer to the first question has a practical aspect – it will tell us whether the grouping of rainbow lenses into doublets results in an advantage in terms of beam parameters. The answer to the second question has a wider implication, due to the connection of obtained rainbow patterns with the general catastrophe theory, enabling one to explore the structural stability of the model proposed [9]. Berry and Upstill [10] have demonstrated that this theory could be used to describe the aberrations of an optical lens in a compact way. It has been also shown that each elementary rainbow pattern obtained with such a lens is related to one of its aberrations [8]. This means that such an approach to the transmission of ion beams through rainbow lenses may also have certain practical consequences.

To this end, we have studied the propagation of protons of a kinetic energy of 10 keV through a square electrostatic rainbow lens doublet. The electrostatic potential in the region of the lens doublet was calculated using a 3-D computer code based on the method of moments [11]. The potential of the electrodes of both lenses was chosen to be 2 kV. The spatial and angular distributions of the initial proton beam were of the Gaussian type.We have analyzed the spatial and angular distributions of the proton beam propagating through the system, as well as the corresponding rainbow lines. The focusing effect of the lens doublet on the beam has been investigated via the parameters determining beam quality.

DOUBLET OF SQUARE ELECTROSTATIC RAINBOW LENSES

In analogy to an electrostatic quadrupole doublet, we introduce a doublet of square electrostatic rainbow lenses. It consists of two coaxial rainbow lenses, axially rotated for 45 degrees relative to each other, as depicted in fig. 1. It has been shown in the previous studies of rainbow lenses [1, 2] that a portion of the ion beam is lost during the transmission due to the radial leaking between the electrodes of the lens.That is why the second lens is rotated axially for 45 degrees relative to the first one – to decrease this effect, at least in the entrance region of the second lens.

The entrance point, midpoint, and exit point of the rainbow lens doublet on the longitudinal axis, *a*, *c* and *e*, respectively, are shown in figs. 1 and 2. At these points, the values of the magnitude of the electrostatic

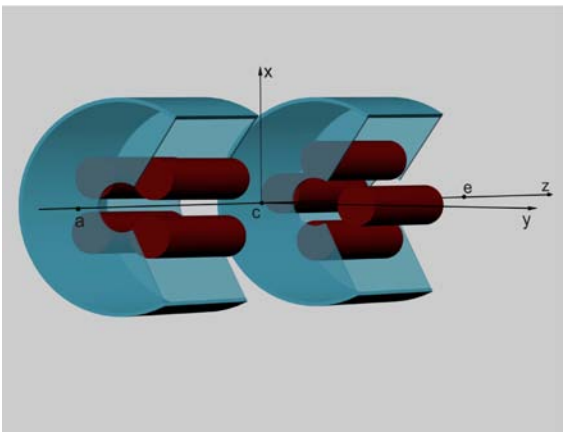

Figure 1. A 3-D view of the rainbow lens doublet; part of the cylindrical housing of the lens doublet is removed to show the arrangement of its electrodes; the regions before point *a* and after the point *e* the are the drift spaces before the first lens and after the second lens, respectively; the transverse position plane including point *c* is the midplane of the lens doublet

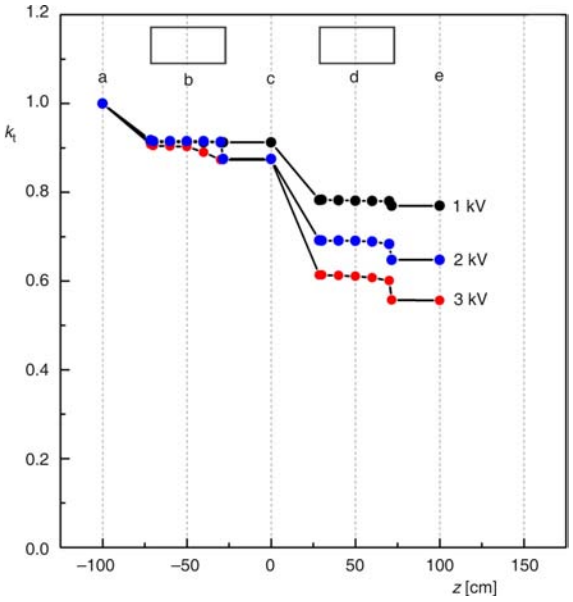

Figure 2. Dependence of the transmission coefficient of the rainbow lens doublet on *z* for φ_0 = 1, 2, and 3 kV; the transverse position planes including points *b* and *d* are the midplanes of the first and second lenses, respectively; the rectangles centered at points *b* and *d* represent the first and second lenses, respectively

field are negligible.The distance between the midpoints of the first and second lenses on the longitudinal axis, b and d, respectively, which are shown in fig. 2, is 1000 mm.

A detailed drawing of a single rainbow lens, together with its dimensions, can be found in [2]. We shall give here only its basic geometric parameters. The diameter and length of the lens electrode are 80 mm and 400 mm, respectively, the distance between the axes of the neighboring electrodes is 120 mm, the diameter and length of the cylindrical housing are 400 mm and 430 mm, respectively, and the diameters of the entrance and exit apertures of the housing are 88 mm.

THEORY

In this study, the *z*-axis of the reference frame is taken to coincide with the axis of the rainbow lens doublet, while the origin coincides with its midpoint (*c*), as depicted in fig. 1. The x- and y-axes of the reference frame are the vertical and horizontal axes, respectively.

Electrostatic field

The electrostatic field of the rainbow lens doublet was constructed using the field map calculated in [4] by applying the appropriate translation and rotation transformations. Unlike the analysis presented in [2], we performed a detailed calculation of the fringe electrostatic fields within the lens doublet. Thus, it was possible to choose the distance between the two lenses in a way that the exit fringe field of the first lens did not interfere with the entrance fringe field of the second lens.

The calculations were performed using the WIPL-D computer code [11]. In such an analysis, the electric field integral equation for the electrodes is solved, *i. e*., the induced current density distribution over their surfaces is determined. This is done by approximating the current density with a series of *N* known basis functions with *N* unknown coefficients and applying the method of moments with the Galerkin test procedure; *N* is the approximation order. Consequently, the integral equation, belonging to the class of linear operator equations, is transformed into a system of *N* linear algebraic equations. This system is solved using the L-U decomposition technique, the results being the values of the unknown coefficients, which give the values of the current density over the electrodes' surfaces at the previously specified grid points. The obtained current density distribution was used to determine the components of the electric field at each point in the region of a lens. Taking into account the symmetry properties of the lens, calculations were performed in the first octant only. The value *N* determining the accuracy of the calculation was 2,913.

Rainbow lines

As in our previous studies of rainbow lenses [1, 2], we are going to apply the theory of crystal rainbows [12-16]. It is based on the singular character of a plane-to-plane mapping associated with the ion transmission process. The mapping involves two transverse planes, perpendicular to the *z*-axis. The former plane is the initial transverse position (TP) plane, including point *a* shown in fig. 1, *i. e*., the impact parameter (IP) plane. The latter plane is the TP plane, including a point between *a* and *e*, shown in fig. 1 and beyond.

Given the dynamical state, *i. e*., the position and velocity vectors of a proton in the IP plane and the electrostatic field within the rainbow lens doublet, one can find its dynamical state in an arbitrary TP plane. This mapping is governed by the corresponding proton equations of motion. One should note that this is five-dimensional mapping, very complex to analyze and visualize. However, it can be reduced to two 2-D mappings in the following manner.

The transverse components of the initial proton position vector are the components of its impact parameter vector, designated as x_0 and y_0. The longitudinal component of the initial proton position vector is designated as z_0. The transverse and longitudinal components of the initial proton velocity vector are designated as v_{x0}, v_{y0}, and v_{z0}, respectively. The obtained transverse components of the proton position vector for the chosen value of *z* are $x(\vec{r}_0, \vec{v}_0, z)$ and $y(\vec{r}_0, \vec{v}_0, z)$, and the corresponding transverse and longitudinal components of the proton velocity vector are $v_x(\vec{r}_0, \vec{v}_0, z)$, $v_y(\vec{r}_0, \vec{v}_0, z)$ and $v_z(\vec{r}_0, \vec{v}_0, z)$, respectively, with $\vec{r}_0 \equiv (x_0, y_0, z_0)$ and $\vec{v}_0 \equiv (v_{x0}, v_{y0}, v_{z0})$. Here, *z* varies from z_0, corresponding to the IP plane, to z_m, corresponding to the final TP plane. Assuming that the proton propagation angle remains small, the corresponding components of the proton transmission angle are $\theta_x(\vec{r}_0, \vec{v}_0, z) = \tan^{-1}(v_x/v_z) \approx v_x/v$ and $\theta_y(\vec{r}_0, \vec{v}_0, z) = \tan^{-1}(v_y/v_z) \approx v_y/v$ where $v(\vec{r}_0, \vec{v}_0, z)$ is the corresponding magnitude of the proton velocity vector. If we consider a parallel proton beam starting at the IP plane, *i. e*., $\theta_x(\vec{r}_0, \vec{v}_0, z_0) = \theta_y(\vec{r}_0, \vec{v}_0, z_0) = 0$, we can define two 2-D mappings. The first one is the mapping of the IP plane to the TP plane, while the second one is the mapping of the IP plane to the transmission angle (TA) plane. The corresponding Jacobians, defined as the ratios of the infinitesimal surfaces in these planes, are

$$J_\rho(\vec{r}_0, \vec{v}_0, z) \equiv \partial_{x0} x \, \partial_{y0} y - \partial_{y0} x \, \partial_{x0} y \quad (1)$$

and

$$J_\theta(\vec{r}_0, \vec{v}_0, z) \equiv \partial_{x0} \theta_x \partial_{y0} \theta_y - \partial_{y0} \theta_x \partial_{x0} \theta_y \quad (2)$$

respectively [1, 2]. Hence, equation $J_\rho(\vec{r}_0, \vec{v}_0, z) = 0$ should give the spatial rainbow lines in the IP plane along which the former mapping is singular. The images of these lines, determined by functions $x(\vec{r}_0, \vec{v}_0, z)$, and $y(\vec{r}_0, \vec{v}_0, z)$, are the rainbow lines in the TP plane. On the other hand, equation $J_\theta(\vec{r}_0, \vec{v}_0, z) = 0$ should give the angular rainbow lines in the IP plane along which the latter mapping is singular. The images of these lines, determined by functions $\theta_x(\vec{r}_0, \vec{v}_0, z)$ and $\theta_y(\vec{r}_0, \vec{v}_0, z)$, are the rainbow lines in the TA plane.

When they appear, the rainbow lines in the TP and TA planes separate the bright and dark regions in these planes. Their shapes are classified by the catastrophe theory [9, 13, 17, 18]. This means that the proton beam dynamics in the rainbow lens doublet has the catastrophic character, as in the case of a single rainbow lens [1, 2]. It has been demonstrated that, for the parallel initial proton beam, the evolution of the spatial and angular distributions of transmitted protons are determined by the evolution of corresponding rainbow patterns [1]. It has also been shown that, for a realistic initial beam, the spatial and angular rainbow lines preserve their confining properties [2]. In this case, the non-parallelism of the beam induces a smearing of the spatial and angular distributions – the rainbow lines are not any longer the sharp boundaries between the bright and dark regions. However, the smearing of the distributions is moderate.

RESULTS AND DISCUSSION

The potential of the electrodes of both lenses of the rainbow lens doublet was chosen to be $\varphi = 2$ kV. The initial proton kinetic energy was 10 keV.The simulation of the proton beam propagation through the lens doublet started from the IP plane, defined by point *a*, shown in fig. 1. An initial beam with vertical and horizontal spatial half-widths of $x_{0m} = y_{0m} = 40$ mm and vertical and horizontal angular half-widths of $\theta_{x0m} = \theta_{y0m} = 5$ mrad, respectively, was considered. We assumed that the beam initially had a double waist, resulting in its vertical and horizontal emittances equal to $\varepsilon_{x0} = \varepsilon_{y0} = \varepsilon_0 = 200$ mm mrad, respectively. The spatial and angular distributions of initial protons were generated from two independent 2-D Gaussian distributions centered at the origins using the common Monte Carlo technique [19]. The standard deviations of the horizontal and vertical spatial and angular distributions were set at $\sigma_x = x_{0m}/2$, $_y = y_{0m}/2$, $\sigma_{\theta x} = \theta_{x0m}/2$ and $\sigma_{\theta y} = \theta_{y0m}/2$, respectively. Proton equations of motion were integrated numerically using the Runge-Kutta method of the fourth order. The space charge forces within the beam were neglected, *i. e.*, the obtained results are valid for small values of the initial proton beam current. The number of protons used in the simulation was $4\ 10^5$. If during the propagation a proton hit a component of the lens, it was excluded from further calculation.

Figure 2 shows the transmission coefficient of the lens, k_t, as a function of z for φ_0 =1, 2, and 3 kV. This coefficient is defined as the ratio of the number of protons reaching the TP plane to the initial number of protons. It is evident that an increase of φ causes a decreases of k_t, as in the case of the single rainbow lens [2]. The values of k_t at point *e* for the chosen values of the electrodes potential are 81.6 %, 68.3 %, and 59 %, respectively. Although one should prefer a higher beam transmission, we have chosen to further study the case of $\varphi = 2$ kV. In this case, the rainbow patterns are more interesting than in the other two cases.

One should note that k_t decreases along the z-axis down to the exit of the second rainbow lens, *i. e.*, for 100 cm z 71.5 cm. Beyond this point, although the fringe electrostatic field of the second lens is not negligible down to z = 100 cm, it remains constant due to the absence of any obstacle that could cause proton beam loss. Maximal beam losses occur at the entrances and exits of the lenses – due to the collisions of protons with the cylindrical housing. At the entrances of the lenses, *i. e.*, for z = –71.5 cm and 28.5 cm, beam losses are 3.2 % and 19.3 %, while at their exits, *i. e.*, for z = –28.5 cm and 71.5cm, they are 4.1 % and 4.0 %, respectively. The beam losses inside the lenses, *i. e.*, for –70 cm z –30 cm and 30 cm z 70 cm, caused by the radial proton leaking between the lens electrodes, amount to 7.2 %.

Spatial and angular distributions

In the field of ion beam transport, the effect of ion focusing is reflected in the osculating and rectifying planes of the central ion trajectory, here being the *xz*- and *yz*-planes, respectively. In this sense, an ion can be either focused or defocused in each of these planes, depending on the sign of the corresponding component of its propagation angle. These cases are denoted as f_x, f_y, d_x, and d_y cases. It is clear that the following four combinations of cases are possible – $f_x f_y$, $f_x d_y$, $d_x f_y$, and $d_x d_y$. In this study, we have used a different definition. If the ion distance from the *z*-axis decreases during its propagation through the rainbow lens doublet, we consider it a focused one. Otherwise, it is a defocused ion. This definition is not connected to any plane. In this case, a focused ion satisfies the condition $xv_x + yv_y$. In the figures given in this paper, the focused and defocused protons are designated by red and green points, respectively (alternative, dark and gray designation colors are used in the printed version of the journal).

In describing the spatial and angular distributions of transmitted protons, we shall present only the results for z 0, *i. e.*, in the region of the second rain-

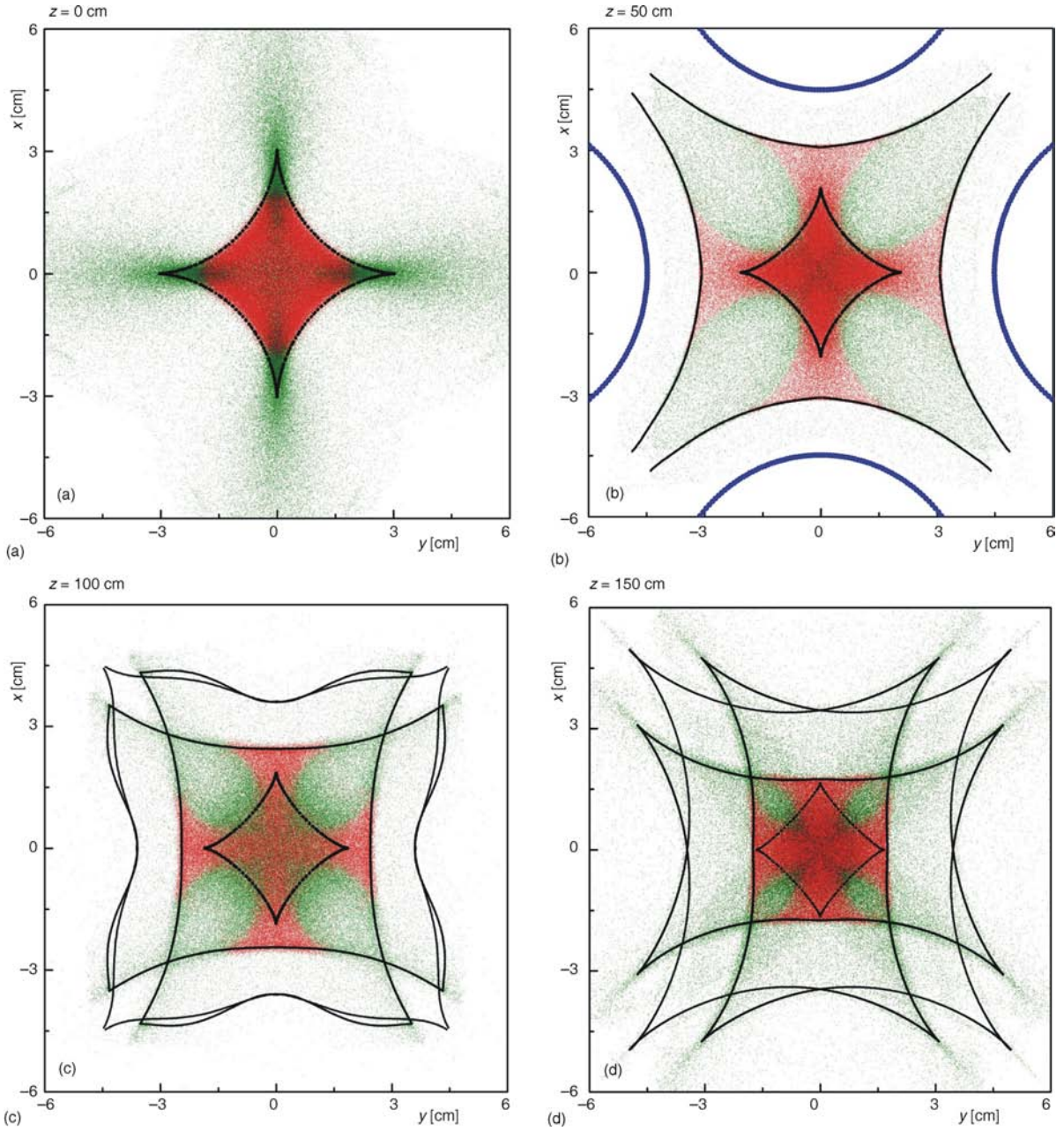

Figure 3. Spatial distributions of the protons transmitted through the rainbow lens doublet for (a) *z* = 0 cm,(b) *z* = 50 cm, (c), *z* = 100 cm, and (d) *z* = 150 cm.The red and green (dark and gray) points designate the focused and defocused protons, respectively; the full black lines are the rainbow lines in the TP plane; the blue (thick black) circular arcs in (b) represent parts of the electrodes of the second lens. (The alternative designation colors refer to the printed version of the journal)

bow lens. Similar results for the first lens have already been presented in [1] and [2].

We shall start our analysis by considering the spatial distributions of transmitted protons for *z* = 0 cm, 50 cm, 100 cm, and 150 cm, given in fig. 3. Figure 3(a) also shows the associated spatial rainbow line, in the TP plane, for *z* = 0 cm, which is a cusped square, sharply dividing the beam core from its halo. By increasing the value of *z*, *i. e*., at a later moment, an additional spatial rainbow line, in the TP plane, appears between the former line and the second rainbow lens electrodes. This is shown in fig. 3(b) where the additional rainbow line has not yet closed and in figs. 3(c) and 3(d), where it becomes a complex closed line containing 12 cusps. We have found that the evolution of this rainbow pattern can be fastened by increasing the lens electrodes potential, as was shown in [1]. According to what has been said in the *Rainbow lines* section, these two rainbow lines are the images of the two rainbow lines in the IP plane, determined by the former mapping. These lines are shown in figs. 4(a-d). The inner and outer lines in the TP plane correspond to the inner and outer lines in the IP plane, respectively. From the catastrophe theory point of view [9], the mapping of the rainbow line given in fig. 4(a) to the rainbow line given in fig. 3(a) can be classified as the mapping governed by a member of the

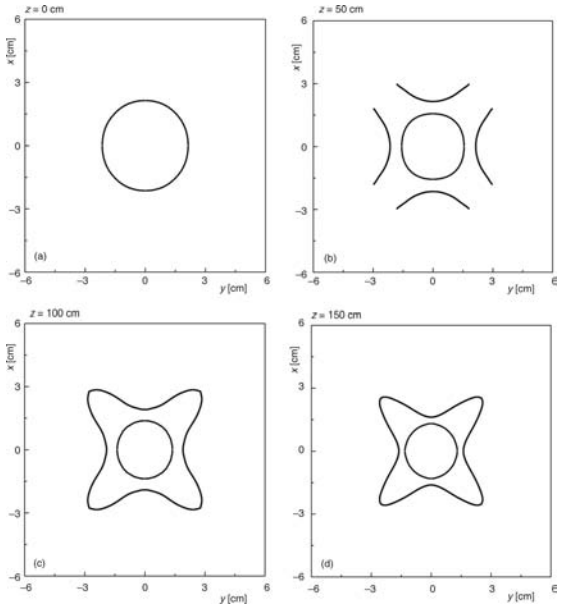

Figure 4. Rainbow lines in the IP plane corresponding to the rainbow lines in the TP plane shown in fig. 3

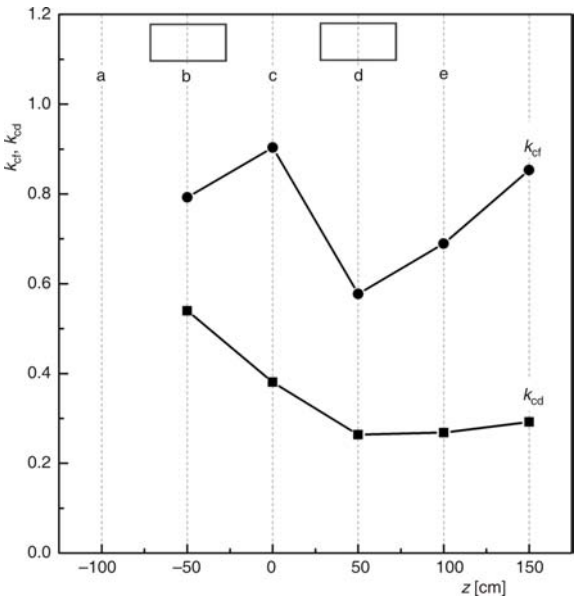

Figure 5. Dependence of the confining coefficients of the rainbow lens doublet for the focused and defocused protons on *z*

$^4X_9$ catastrophe family [17, 20]. The classification of the mappings of the other lines given in fig. 4 to the lines given in fig. 3 by catastrophe theory requires additional serious study.

One should note that the protons in the vicinity of a rainbow line in one TP plane, for one value of *z*, do not coincide with the protons in the vicinity of the same line in another TP plane, for another value of *z*. Besides, the appearance of the latter rainbow line in the TP plane causes a redistribution of ions in this plane – the former line confines the major part of the proton beam and the latter line confines most of the remaining part of the beam. This means that the number of ions outside the latter rainbow line is negligible, forming the beam halo. The same is true for the rainbow lines for $z > 100$ cm, *i. e.*, in the drift space after the second rainbow lens, as can be seen in fig. 3(d). When the value of *z* increases beyond this value, the extent of the inner rainbow line decreases, but without a tendency of a reduction to a point. This behavior is attributed to the anharmonic character of the electrostatic potential of the lens doublet, as in the case of the single rainbow lens [1].

In order to quantify the effect of proton beam confinement by the rainbow lens doublet, we shall use the coefficients introduced for a single rainbow lens [1], the confining coefficients of the focused and defocused protons, k_{cf} and k_{df}, respectively. Coefficient k_{cf} is the ratio of the number of focused protons confined within the inner rainbow line, *i. e.*, within the proton beam core, to the total number of focused protons in the TP plane, while k_{df} is the number of defocused protons confined within the inner line to the total number of defocused protons in the TP plane. The dependencies of these coefficients on *z* are given in fig. 5. They are maximal for $z = 0$ cm, when only the inner rainbow line exists. For $z > 0$, k_{cf} decreases, exhibiting a minimum for *z* around 50 cm, and increasing to a value close.5 yet below the maximal one. The minimal value of k_{cf} corresponds to the moment when the outer rainbow line closes, coinciding with the moment when the number of protons leaving the beam core becomes maximal. The subsequent increase of k_{cf} occurs due to a decrease of the total number of focused protons, particularly outside the beam core, *i. e.*, due to their conversion to the defocused protons. This is especially pronounced in the region of the fringe electrostatic field, where the focusing power of the second lens is weak, and in the drift space after the second lens. The value of k_{cf} for $z = 0$ cm is 90.4 %, while for $z = 100$ cm, *i. e.*, at the exit of the lens doublet, it is 68.9 %. Figure 5 also shows that for $z > 0$, k_{df} decreases, attaining a minimum for *z* around 50 cm, and slightly increasing to a value below the maximal one. The fact that this increase is slight can be attributed to a permanent increase of the number of defocused protons leaving the beam core. The value of k_{df} for $z = 0$ cm is 38.1 % while for $z = 100$ cm, *i. e.*, at the exit of the lens doublet, it is 26.8 %.

We have also analyzed the rainbow lines in the TA plane. These lines determine the angular distributions of transmitted protons for different values of *z* in a similar way as the rainbow lines in the TP plane determine the spatial distributions of transmitted protons. This is illustrated in figs. 6(a, b) depicting the angular distributions of transmitted protons and the associated rainbow lines for $z = 50$ cm and 100 cm. Figure 7(a, b) shows the corresponding rainbow lines in the IP plane. We believe that the classification of the mappings of the rainbow lines shown in fig. 7 to the lines shown in fig. 6 represent an intriguing subject from the catastrophe theory point of view.

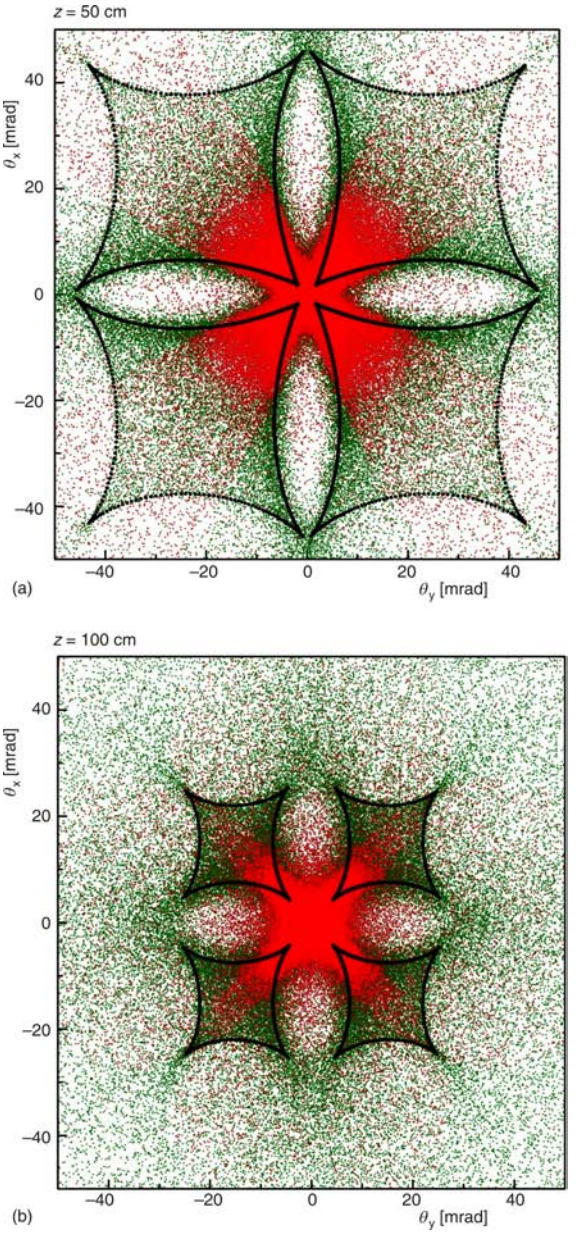

Figure 6. Angular distributions of the protons transmitted through the rainbow lens doublet for (a) z = 50 cm and (b) z = 100 cm; the red and green (dark and gray) points designate the focused and defocused protons, respectively; the full black lines are the rainbow lines in the TA plane. (The alternative designation colors refer to the printed version of the journal)

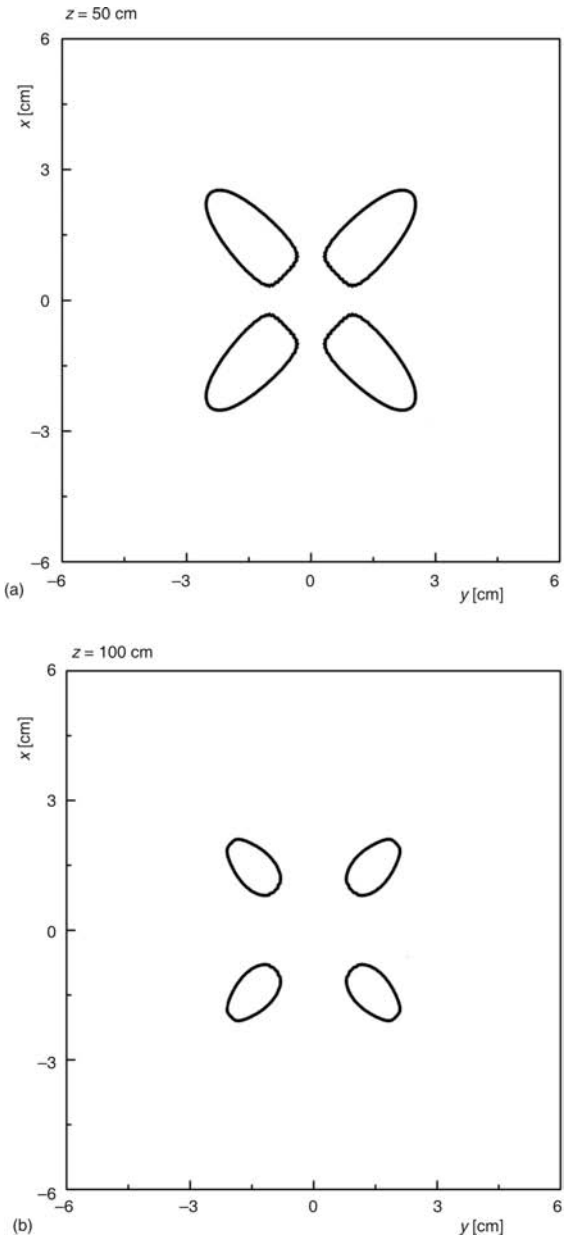

Figure 7. Rainbow lines in the IP plane corresponding to the rainbow lines in the TA plane shown in fig. 6

The distributions of transmitted protons in the $x\theta_x$ or $y\theta_y$ plane, *i. e.*, the phase-space portraits of the proton beam for different values of z have also been studied. It was determined that the action of the rainbow lens doublet on the beam is highly non-linear, as in the case of the single rainbow lens [2].

Beam parameters

In this section we shall consider several parameters that characterize the quality of the proton beam transmitted through the rainbow lens doublet. Figure 8 shows the focusing coefficient of the lens doublet, k_f, as a function of z between 100 cm and 150 cm. This parameter is the ratio of the number of focused protons in a TP plane to the initial number of protons [1, 2]. In general, k_f decreases with z. However, in the regions immediately before the entrances and exits of the lenses, k_f sharply decreases and increases, respectively. This is attributed to the fact that in the former region, the protons are decelerated and, thus, defocused, and that in the latter region, they are accelerated and, thus, focused. This effect was observed in the case of the single rainbow lens [2].

Figure 9 gives the ratio of the density of the proton beam core to the initial beam density, $\eta_c\,\eta$, the ratio of the vertical or horizontal emittance of the beam core to the initial vertical or horizontal beam emittance, $\varepsilon_c/\varepsilon$,

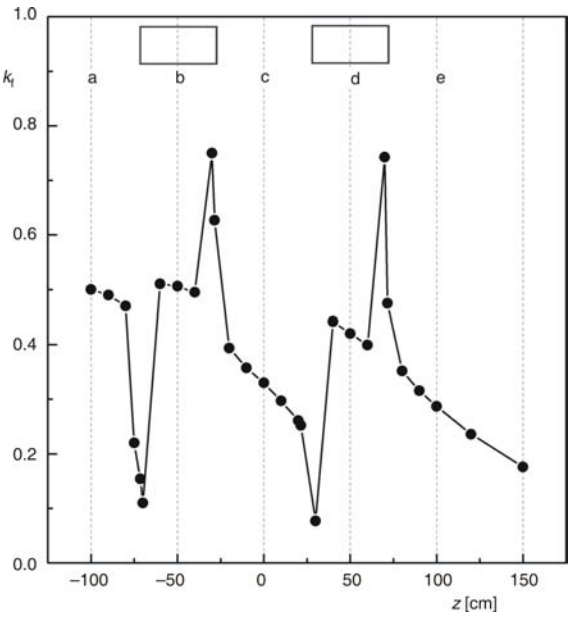

Figure 8. Dependence of the focusing coefficient k_f of the rainbow lens doublet on *z*; the region after point *e* is the drift space after the second lens; the TP plane including point *c* is the midplane of the lens doublet; the TP planes including points *b* and *d* are the midplanes of the first and second lenses, respectively; the rectangles centered at points *b* and *d* represent the first and second lenses, respectively

and the ratio of the brightness of the beam core to the initial beam brightness, B_c/B_0, as a function of *z* between –50 cm and 150 cm. The three normalizing values are the same as in [2], *i. e.*, $\eta_0 = 79$ mm^{-2}, $\varepsilon_0 = 200$ mmmrad, and $B_0 = = 1.62\ 10^{-8}$ A/mm^2 mrad^2. In calculating the values of B_0 and B_c, we assumed that the incoming protons formed a beam bunch of a length of 10 ms. The resulting initial beam current was 6.4 nA.

These dependences show that η_c has a maximum for z = 100 cm, reaching the value of 1083 mm^{-2}, which is 13.7 times larger than η_0. Further, ε_c decreases in the entire considered *z* region. At the exit of the rainbow lens doublet, for z = 100 cm, the parameter 104.6 mmmrad, is 1.9 times smaller than ε_0. At the chosen end of the drift space after the second lens, for z = 150 cm, ε_c, being 86.6 mmmrad, it is 2.3 times smaller than ε_0. Finally, B_c increases throughout the whole considered *z* region. At the lens doublet exit, this parameter being $1.48\ 10^{-8}$ A/mm^{2}mrad^2, it is 1.1 times smaller than B_0. At the chosen end of the drift space after the second lens, B_c, being $1.48\ 10^{-8}$ mA/mm^{2}mrad^2, is 1.37 times larger than B_0. When one compares these values with the corresponding ones obtained in the case of the single rainbow lens treated in [2], it is evident that, in this case, the density of the beam core is about 30 % lesser, while its emmitance and brightness do not differ significantly.

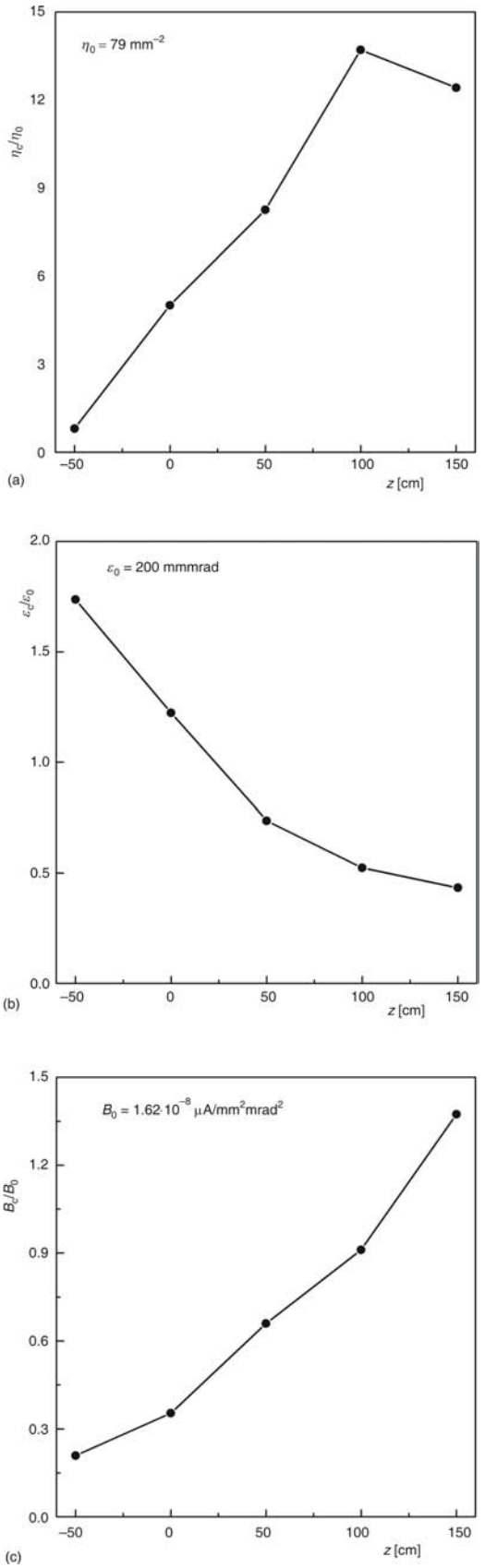

Figure 9. Dependences of (a) the density of the proton beam core to the initial beam density, (b) the ratio of the vertical or horizontal emittance of the beam core to the initial vertical or horizontal beam emittance, respectively, and (c) the ratio of the brightness of the beam core to the initial beam brightness on *z*

CONCLUSIONS

In order to study the focusing properties of the rainbow lens doublet, we have simulated the propagation of a 10 keV proton beam along this optical element. The potential of the electrodes of the lenses has been chosen to be 2 kV. We have investigated the spatial and angular ditributions of transmitted protons together with the corresponding rainbow lines and parameters defining the proton beam quality.The results have been analyzed only in the region of the second lens and in the drift space after it, since the corresponding results for a single rainbow lens were presented in [1, 2].

As in the case of the single rainbow lens, analysis has shown that there is a spatial rainbow line exhibiting a strong confining property which leads to the formation of a proton beam core, defined by the line itself. However, in this case, when compared with the case of the single lens, the evolution of the rainbow pattern differs – an additional rainbow line occurs, exhibiting a weaker confining property than the former one. The latter rainbow line defines the outer border of the beam. It has been also established that the spatial rainbow patterns determine the shapes of the spatial distributions of transmitted protons which appear as the skeletons of the said distributions. The same is true for the angular rainbow patterns and the angular distributions of transmitted protons.

In a TP plane, the spatial rainbow line that appears first is a cusped square. It is the image of a circle-like line in the IP plane. From the catastrophe theory point of view, the mapping of the line in the IP plane to the one in the TP plane is governed by a member of the ${}^4X_9$ catastrophe family. The classification of the mappings of additional spatial rainbow lines and angular rainbow lines will be the subject of a separate study. That study should relate to the problem of the aberrations of the rainbow lens doublet.

Our analysis of the parameters that characterize the beam quality of the proton beam regarding its efficient transport through a transport line or its interactions with a target in an experimental set-up has shown that the actions of the rainbow lens doublet do not differ considerably from the action of a single rainbow lens. The action of the lens doublet is comparable with the action of a single lens of the corresponding length.

ACKNOWLEDGMENT

We would like to acknowledge the support of the Ministry of Education, Science and Technological Development of the Republic of Serbia provided to us through the project Physics and Chemistry with Ion Beams, No.III45006.

AUTHORS' CONTRIBUTIONS

The idea for this research was initiated by N. B. Nešković. Computations were carried out by I. N. Telečki and P. D. Beličev. The manuscript was written by P. D. Beličev, N. B. Nešković, I. N. Telečki, and S. M. Petrović.

REFERENCES

[1] Nešković, N., *et al*., A Square Electrostatic Rainbow Lens: Catastrophic Ion Beam Focusing, *Nucl. Instr. Meth. Phys. Res., A 635* (2011), 1, pp. 1-7
[2] Telečki, I., *et al*., Focusing Properties of a Square Electrostatic Rainbow Lens, *Nucl. Instr. Meth. Phys. Res., A 694* (2012), Dec., pp. 224-233
[3] Ristić-Djurović, J. L., *et al*., Optimization of Equally Charged Quadrupole Parameters, *IEEE Trans. Nucl. Sci., 60* (2013), 3, pp. 2161-2169
[4] Nešković, N., *et al.*, Rainbow Lenses, Advances in Imaging and Electron Physics (Academic Press, Waltham, 2014), Vol. 182, pp. 123-186
[5] Ristić-Djurović, J. L., *et al*., Ion Beam Acceleration with Radio Frequency Powered Rainbow Lens, *IEEE Trans. Nucl. Sci., 60* (2013), 2, pp. 1272-1279
[6] De Hoffmann, E., Stroobant, V., Mass Spectrometry, Wiley & Sons, Chichester, UK, 2007
[7] Septier, A., Focusing of Charged Particles, Academic Press, New York, 1967
[8] Rose, H., Geometrical Charged-Particle Optics, Springer-Verlag, Heidelberg, 2013
[9] Thom, R., Structural Stability and Morphogenesis, Benjamin, Reading, 1975
[10] Berry, M. V., Upstill, C., Catastrophe Optics: Morphologies of Caustics and Their Diffraction Patterns, Progress in Optics XVIII (North-Holland, Amsterdam, 1980), pp. 257-346
[11] ***, WIPL-D, 3-D Electromagnetic Solver Professional Edition (WIPL-D, Belgrade, 2009)
[12] Nešković, N., Rainbow Effect in Ion Channeling, *Phys. Rev., B33* (1986), 9, pp. 6030-6035
[13] Nešković, N., Perović, B., Ion Channeling and Catastrophe Theory, *Phys. Rev. Lett., 59* (1987), 3, pp. 308-310
[14] Petrović, S., *et al*., Theory of Rainbows in thin Crystals: the Explanation of Ion Channeling Applied to Ne^{10+} Ions Transmitted Through a <100> Si thin Crystal, *Phys. Rev., B61* (2000), 1, pp. 184-189
[15] Nešković, N., *et al*., Rainbows in Channeling of 1 GeV Protons in a Bent Very Short (11, 9) Single-Wall Carbon Nanotube, *Int. J. Nonlinear Sci. Numer. Simul., 11* (2010), 12, pp. 1131-1143
[16] Borka, D., *et al*., Channeling of Protons Through Carbon Nanotubes, Nova Science, NewYork, 2011
[17] Nešković, N., *et al*., The X9 Catastrophe as the Organizing Center of Crystal Rainbows, *Phys. Lett., A 179* (1993), pp. 343-347
[18] Nešković, N., *et al*., Crystal Rainbows in the Cases of Square Very thin Crystals with one Atomic String Per Primitive Cell, *Nucl. Instrum. Meth. Phys. Res., B 93* (1994), 3, pp. 249-251
[19] Lund, S. M., *et al.*, Generation of Initial Kinetic Distributions for Simulation of Long-Pulse Charged Particle Beams with High Space-Charge Intensity, *Phys. Rev. ST Accel. Beams, 12* (2009), p. 114801
[20] Nye, J. F., Natural Focusing and Fine Structure of Light, Institute of Physics, Bristol, UK, 1999, p. 193

Received on October 19, 2015
Accepted on November 26, 2015

Игор Н. ТЕЛЕЧКИ, Петар Д. БЕЛИЧЕВ, Срђан М. ПЕТРОВИЋ, Небојша Б. НЕШКОВИЋ

ДУБЛЕТ ДУГИНИХ СОЧИВА

У раду се анализирају карактеристике дублета електростатичких квадратних дугиних сочива. Овај јонско-оптички елемент садржи два електростатичка квадратна дугина сочива, једно у односу на друго аксијално ротирано за 45°. Анализиран је транспорт снопа протона енергија 10 keV кроз овај јонско-оптички елемент. Једносмерни напон на електродама оба сочива дублета износи 2 kV. Електростатички потенцијал и одговарајуће компоненте електричног поља израчунате су помоћу рачунарског кода заснованог на методи момената. Анализиране су просторне и угаоне расподеле протона у дублету као и параметри који дефинишу квалитет снопа. Као и у случају појединачног електростатичког квадратног дугиног сочива, еволуција ових расподела је одређена одговарајућом еволуцијом линија дуга, које су генерисане на бази теорија кристалних дуга. Анализа показује да се језгро снопа, које има облик криволинијског квадрата са теменима у облику рога, формира око просторне дуге која се прва појављује. Ова линија дуге формира се у првом сочиву дублета. Језгро снопа остаје унутар поменутог криволинијског квадрата и за време пропагације кроз друго сочиво дублета. Електростатичко поље у другом сочиву узрокује појављивање додатне линије дуге, која обухвата језгро снопа и дефинише спољну границу снопа. Појављивање ове линије чини главну разлику између ефеката који на сноп врше појединачно сочиво и дублет.

Кључне речи: електростатичко сочиво, динамика честичног снопа, протонски сноп